ELSEVIER

International Journal of Heat and Fluid Flow 23 (2002) 758–765

International Journal of HEAT AND FLUID FLOW

www.elsevier.com/locate/ijhff

Turbulent mixed convection flow over a backward-facing step—the effect of the step heights

H.I. Abu-Mulaweh [a,*], T.S. Chen [b], B.F. Armaly [b]

[a] Mechanical Engineering Department, Purdue University at Fort Wayne, 2101 E. Coliseum Blvd., Fort Wayne, IN 46805, USA
[b] Department of Mechanical and Aerospace Engineering and Engineering Mechanics, University of Missouri-Rolla, Rolla, MO 65409, USA

Received 10 January 2002; accepted 15 May 2002

Abstract

Effect of the backward-facing step heights on turbulent mixed convection flow along a vertical flat plate is examined experimentally. The step geometry consists of an adiabatic backward-facing step, an upstream wall and a downstream wall. Both the upstream and downstream walls are heated to a uniform and constant temperature. Laser–Doppler velocimeter and cold wire anemometer were used, respectively, to measure simultaneously the time-mean velocity and temperature distributions and their turbulent fluctuations. The experiment was carried out for step heights of 0, 11, and 22 mm, at a free stream air velocity, u_∞, of 0.41 m/s, and a temperature difference, ΔT, of 30 °C between the heated walls and the free stream air. The present results reveal that the turbulence intensity of the streamwise and transverse velocity fluctuations and the intensity of temperature fluctuations downstream of the step increase as the step height increases. Also, it was found that both the reattachment length and the heat transfer rate from the downstream heated wall increase with increasing step height.

1. Introduction

Flow separation and recirculation caused by a sudden change in flow geometry, such as a backward-facing step, play an important role in the design of a wide variety of heat transfer devices, such as cooling systems for electronic equipment, combustion chambers, high performance heat exchangers, chemical process equipment, environmental control systems, and cooling passages in turbine blades. A significant amount of mixing of high and low energy fluid occurs in the reattached flow region in these devices, thus affecting their heat transfer performance. The problem of laminar flow over a backward-facing step geometry in natural, forced, and mixed convection has been investigated rather extensively in the past, both numerically and experimentally (see, for example, Lin et al. (1990), Hong et al. (1993) and Abu-Mulaweh et al. (1995) and the references cited therein). On the other hand, studies of turbulent flow over a backward-facing step have dealt mainly with forced and natural convection cases (see, for example, Vogel and Eaton (1985), Inagaki (1994), Abe et al. (1994, 1995), Park and Sung (1995), Rhee and Sung (1996) and Abu-Mulaweh et al. (1999) and the references cited therein). Recently, Abu-Mulaweh et al. (2001) investigated the effects of free stream velocity on turbulent natural convection over a backward-facing step. In the present study consideration is given to buoyancy-dominated mixed convection over a two-dimensional, vertical backward-facing step to examine the effect of step heights on turbulent mixed convection. The step geometry consists of an adiabatic step and upstream and downstream walls that are heated to a constant and uniform temperature.

Results of interests such as time-mean velocity and temperature, intensities of velocity and temperature fluctuations, and local Nusselt number distributions are reported to illustrate the effect of step heights on the flow and thermal fields characteristics of turbulent mixed convection downstream of a backward-facing step. Such detailed results are needed for optimizing the performance of heat transfer devices, and for developing or validating models for simulating their behaviors.

* Corresponding author. Tel.: +1-260-481-6357; fax: +1-260-481-5728.
E-mail address: mulaweh@ipfw.edu (H.I. Abu-Mulaweh).

0142-727X/02/$ - see front matter © 2002 Elsevier Science Inc. All rights reserved.
PII: S0142-727X(02)00191-1

Nomenclature

AR	aspect ratio, W/s
ER	expansion ratio, H/s
Gr_x	local Grashof number, $g\beta\ (T_w - T_\infty)x^3/v^2$
g	gravitational acceleration
h	local heat transfer coefficient, $-k(\partial T/\partial y)_{y=0}/(T_w - T_\infty)$
H	distance between the heated downstream wall and the unheated wall of the tunnel
k	thermal conductivity
Nu_{x^*}	local Nusselt number, hx^*/k
s	step height
T	fluid temperature
T_∞	free stream temperature
T_w	wall temperature
$\overline{t'^2}$	intensity of temperature fluctuations
u	mean streamwise velocity
u_∞	free stream velocity
u^*	reference velocity, $[g\beta(T_w - T_\infty)x_i]^{1/2}$
$\overline{u'^2}$	intensity of streamwise velocity fluctuations
$\overline{u't'}$	streamswise turbulent heat flux
U	dimensionless mean streamwise velocity, u/u^*
v	mean transverse velocity
$\overline{v'^2}$	intensity of transverse velocity fluctuations
$\overline{v't'}$	transverse turbulent heat flux
V	dimensionless mean transverse velocity, v/u^*
W	width of plate
x, y	streamwise and transverse coordinates measured from the downstream plate
x^*	$x + x_i$
x_i	inlet length upstream of the step
x_r	reattachment length
y^*	$y - s$
Greeks	
β	Coefficient of thermal expansion
ΔT	temperature difference, $(T_w - T_\infty)$
θ	dimensionless temperature, $(T - T_\infty)/(T_w - T_\infty)$
v	kinematic viscosity

2. Experimental apparatus and procedure

The experimental investigation was performed in an existing low turbulence, open circuit air tunnel that was oriented vertically, with air flowing in the upward direction. Details of the air tunnel has been described by Abu-Mulaweh et al. (1999) and a schematics of the tunnel is shown in Fig. 1. It has a smooth converging nozzle, a straight square test section, and a smooth diverging diffuser. Plastic honeycomb and stainless steel screens are placed at the inlet of the air tunnel to straighten the flow and to minimize the free stream turbulence in the test section. A variable-speed suction fan is attached to the end of the diffuser section. The tunnel is constructed from a 1.27 cm thick plexiglass plate and a 1.91 cm plywood with adequate steel frames and supports to provide a rigid structure. The test section, which is constructed from transparent plexiglass material, allows for flow visualizations and permits the use of a laser–Doppler velocimeter (LDV) for velocity measurements. The step geometry is supported in the test section of the tunnel and spans its entire width (85.1 cm). A cross section of 63.5×85.1 cm is provided adjacent to the test surface in the test section for the developing boundary layer air flow.

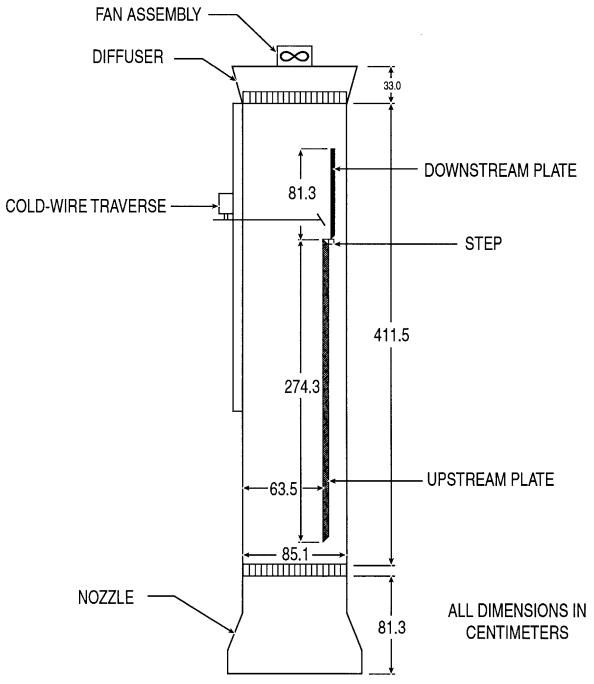

Fig. 1. Schematic diagram of the air tunnel.

Fig. 2 shows a schematic diagram of the step geometry which consists of an adiabatic backward-facing step, an upstream wall (274.3 cm in length), and a downstream wall (81.3 cm in length). Both the upstream and the downstream walls can be heated to a constant and uniform temperature. The heated walls are made of three composite layers that are held together by screws. The upper layer is an aluminum plate (85.1 cm wide, and 1.27 cm thick) instrumented with several thermocouples that are distributed in the axial direction along its entire length. Each thermocouple is inserted into a small hole from the backside of the plate and its measuring junction is flush with the test surface. The middle layer

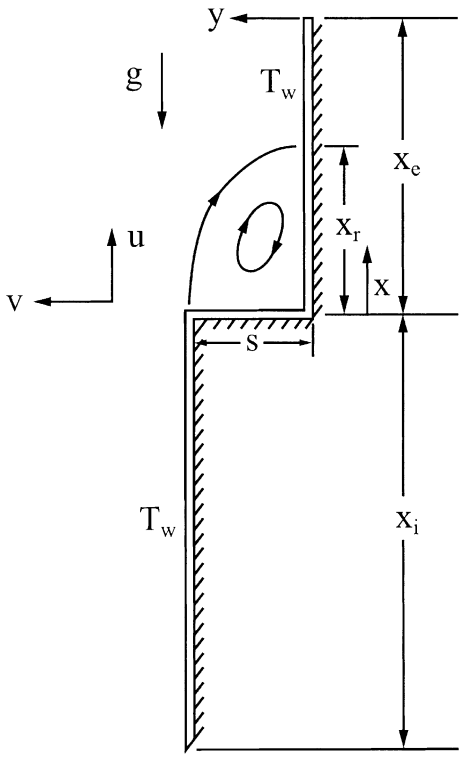

Fig. 2. Schematic diagram of the step geometry.

consists of several heating pads that can be controlled individually for electrical energy input. By controlling the level of electrical energy input to each of the heating pads, and monitoring the local temperature of the heated walls with the imbedded thermocouples, the temperature of the heated surface can be maintained constant and uniform to within 0.2 °C. The bottom layer of the heated walls is a 1.91-cm thick plywood board serving as backing and support for the heated wall structure. The backward-facing step is made of Plexiglass to simulate an adiabatic surface. The front edge of the upstream plate is chamfered to insure a proper development of the boundary layer flow. The edges of the upstream and downstream walls which are in contact with the step, are also chamfered to minimize the contact area, and hence the conduction heat transfer, between the heated walls and the adiabatic step, as shown in Fig. 1.

Air velocity and temperature were measured simultaneously by using a two-component LDV and a cold wire anemometer, respectively. The LDV system is equipped with an automated three dimensional traverse system for positioning the measuring LDV probe volume at any desired point in the flow domain. The cold wire probe with a separate traverse system is placed within 2 mm behind the measuring LDV volume. The outputs from both the LDV and the cold wire anemometer are then processed through an A/D converter and a suitable software on an IBM personal computer to determine the local instantaneous velocity and temperature. These measurements were then used to determine the time-mean velocity and temperature, intensities of velocity and temperature fluctuations, and local Nusselt number distributions.

It was established, through repeated LDV measurements, that 1024 acceptable LDV samples of the local instantaneous fluctuating velocity component were sufficient to repeatedly and accurately determine the local mean velocity and temperature in the flow domain. The acceptable sampling rate for these measurements varied between 10 and 100 sample/s. All of the reported data in this study resulted from taking the average of two separate measurements taken back to back, each of which having a sample of 1024 instantaneous measurements.

The repeatability of the mean velocity measurements was determined to be within 4%, and that of the temperature measurements was within 0.25 °C (0.5%). The uncertainties in the measured results were estimated (at the 95% confidence level) according to the procedure outlined by Moffat (1988) and they are reported in the appropriate section of this paper.

Flow visualizations were also performed to verify the boundary-layer development and its two-dimensional nature. These flow visualizations were carried out by using a 15-W collimated white light beam, 2.5 cm in diameter. Glycerin smoke particles, 2–5 μm in diameter, which are generated by immersing a 100 W heating element into a glycerin container, are added to the inlet air flow and used as scattering particles for flow visualization and for LDV measurements.

3. Results and discussion

The boundary layer development in the experimental set up, along with its two dimensional nature, was verified through flow visualization and through measurements of velocity across the width of the tunnel, at various heights above the heated wall. These measurements showed a wide region (about 80% of the width of the heated wall around its center) where the air flow velocity is almost constant (to within 5%) at a fixed distance from the heated surface, thus justifying the two-dimensional flow approximation. It should be noted that in the present experimental study two step heights were examined $s = 11$ and 22 mm (corresponding to expansion ratios of 58.7 and 29.9, and aspect ratios of 77.4 and 38.7, respectively). In addition, velocity measurements in the free stream were performed (up to 200 mm from the edge of the boundary layer) and showed that the free stream velocity is uniform and constant (to within 2%). The operation of the air tunnel, its instrumentation, and the accuracy and the repeatability of the measurements were validated by performing measurements of turbulent natural convection boundary-layer

flow adjacent to a vertical heated flat plate at a uniform temperature in the air tunnel for different levels of heating conditions. Both the measured flow and thermal fields compared well with other previously measured and predicted results, as was reported by Abu-Mulaweh et al. (1999). All reported measurements were taken along the midplane ($z = 0$) of the plate's width, and only after the system had reached steady state conditions.

Measurements of the flow field were carried out at a location upstream of the step ($x = -5$ cm) for pure forced convection flow ($u_\infty = 0.41$ m/s, $\Delta T = 0$ °C), pure natural convection flow ($u_\infty = 0$ m/s, $\Delta T = 30$ °C), and mixed convection flow ($u_\infty = 0.41$ m/s, $\Delta T = 30$ °C) for comparison. This comparison is presented in Figs. 3 and 4. The dimensionless streamwise velocity distributions, shown in Fig. 3, follow the expected shape and behavior for these cases. It can be seen that there is a velocity overshoot in the mixed convection case, due to the buoyancy assisting. The effect of free stream velocity on the velocity fluctuations is illustrated in Fig. 4. The figure shows that the introduction of free stream velocity on the turbulent natural convection flow reduces the level of turbulence intensity inside the boundary layer. This results in a suppressed turbulent mixed convection regime. These trends are similar to those reported by Abu-Mulaweh et al. (2000) and Hattori et al. (2001). The uncertainties in these measurements are ±0.1 mm in y^*, ±4% in U and ±6% in $\sqrt{\overline{u'^2}}/u^*$.

To examine the effect of step heights on the flow and thermal fields of turbulent mixed convection flow, measurements of the flow and thermal fields were carried out at four different streamwise locations downstream of the step ($x = 3.5$, 6, 10, and 25 cm), at a free stream velocity of 0.41 m/s, for three different step heights $s = 0$ mm (flat plate) and $s = 11$ and 22 mm (corresponding to Reynolds number, $Re_s = u_\infty s/\nu$, of 278.4 and 556.8, respectively), and a temperature difference of 30 °C between the heated walls and the free stream.

The dimensionless time-mean streamwise and transverse velocity and temperature distributions downstream of the step ($x = 3.5$, 6, 10, and 25 cm) are presented in Figs. 5–7, respectively. These figures illustrate the effect of step heights on the turbulent mixed

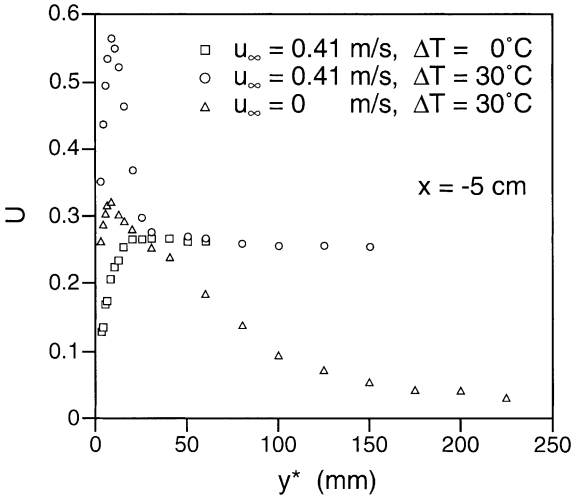

Fig. 3. Dimensionless mean streamwise velocity distributions upstream of the step.

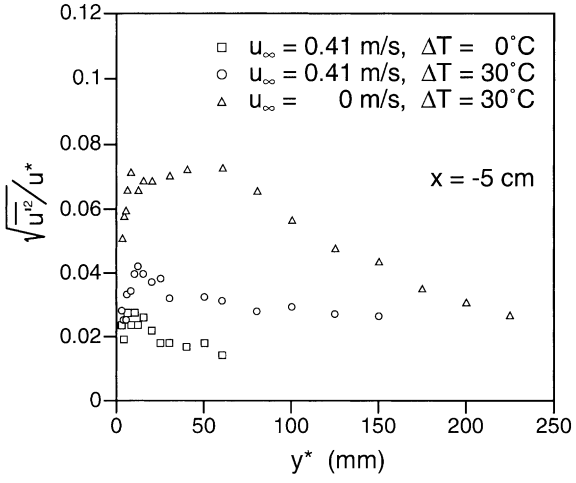

Fig. 4. Distributions of dimensionless streamwise velocity fluctuation upstream of the step.

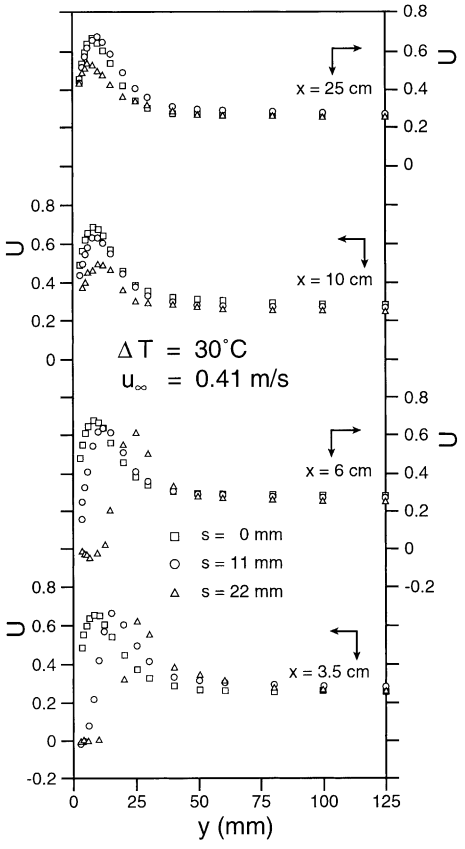

Fig. 5. Dimensionless mean streamwise velocity distributions downstream of the step.

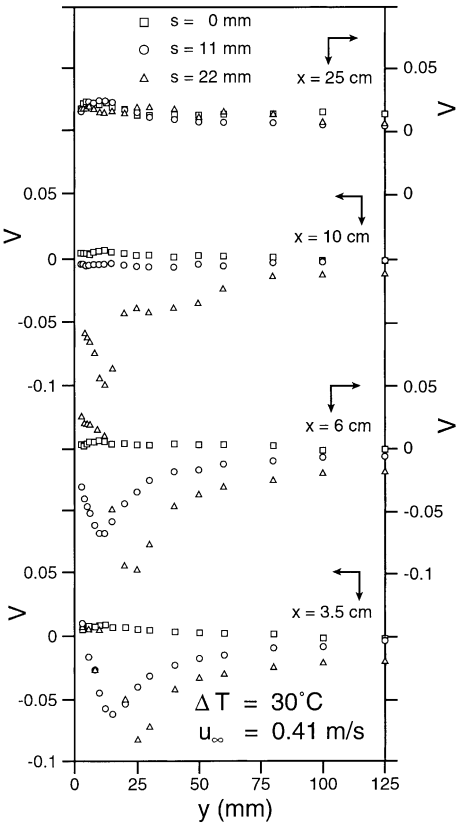

Fig. 6. Dimensionless mean transverse velocity distributions downstream of the step.

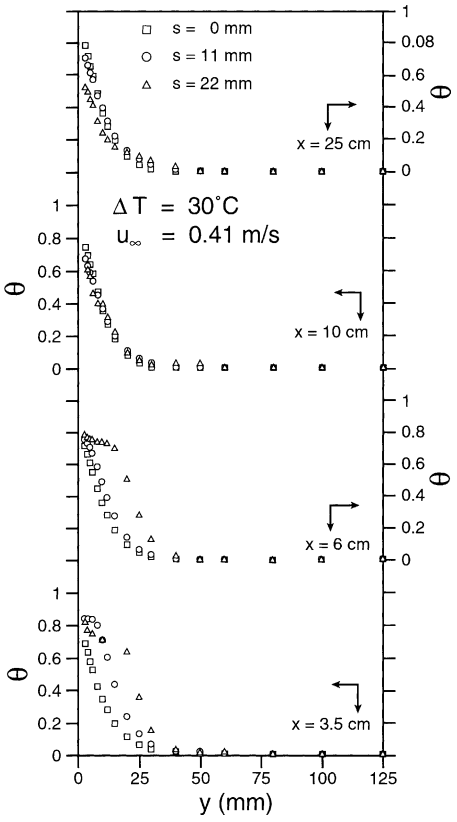

Fig. 7. Dimensionless mean temperature distributions downstream of the step.

convection downstream from the step. Fig. 5 shows that the velocity profiles at $x = 3.5$ and 6 cm exhibit negative mean streamwise velocity component for the case of step heights of $s = 11$ and 22 mm. This is because of the introduction of backstep in the flow geometry which causes a separation at the upper corner of the step creating a recirculation region downstream of the step. It was observed that the length of this recirculation region increases with increasing step height. It was determined that for the experimental conditions shown in Fig. 5, the reattachment lengths are $x_r = 6.5$ cm and 9.5 cm (or $x_r/s = 5.9$ and 4.38) for the step heights of $s = 11$ and 22 mm, respectively. The reattachment length was measured from flow visualization. The reported reattachment length measurements represent the average of many readings that were obtained under a fixed condition in order to reduce visualization errors. The uncertainty in these measurements is ±1 mm. It should be noted that the velocity profile for the turbulent mixed convection for the case of step height $s = 11$ mm, the streamwise location x = 6 cm is inside the recirculation region ($x_r = 6.5$ cm). The reason for the velocity profile not to exhibit negative velocity component is that the thickness of the recirculation region is very thin at this streamwise location, where the first measured experimental data point is at 3 mm from the heated wall. The figure also shows the effect of step on the flow field continues to be present even at large distances downstream from the step ($x = 25$ cm), especially for large step heights ($s = 22$ mm).

Fig. 6 shows that for cases of backward-facing step ($s = 11$ and 22 mm) the distributions at $x = 3.5$, 6, and 10 cm exhibit negative mean transverse velocity component in the region near the heated surface. The reason for the negative mean transverse velocity component is because of the sudden expansion in the flow geometry which causes the streamlines to curve towards the downstream heated surface. However, the profiles at $x = 25$ cm do not exhibit any negative mean transverse velocity component near the heated surface, indicating that the effect of the backward-facing step has been diminished. The magnitude of the negative mean transverse velocity component increases with increasing step height. This is because curvature of the streamlines towards the downstream heated surface is steeper for larger steps. Fig. 7 presents the dimensionless temperature distributions downstream of the step for different step heights. This figure shows that the step height affects the characteristics of the thermal field downstream of the step. The uncertainties in these measurements are ±0.1 mm in y, ±4% in U and V and ±2% in θ.

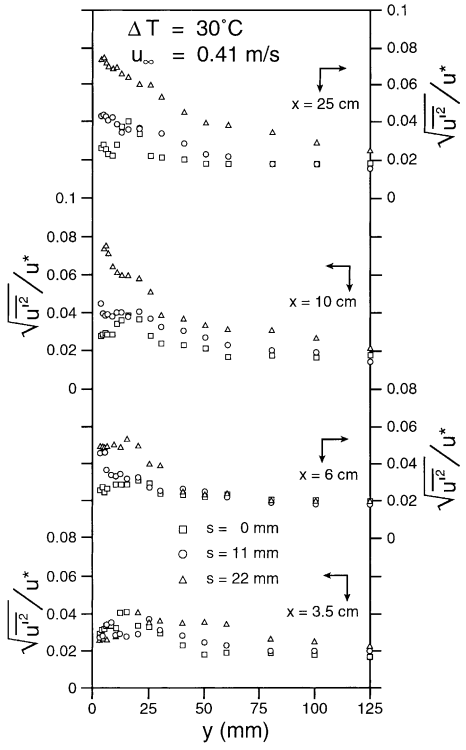

Fig. 8. Distributions of dimensionless streamwise velocity fluctuation downstream of the step.

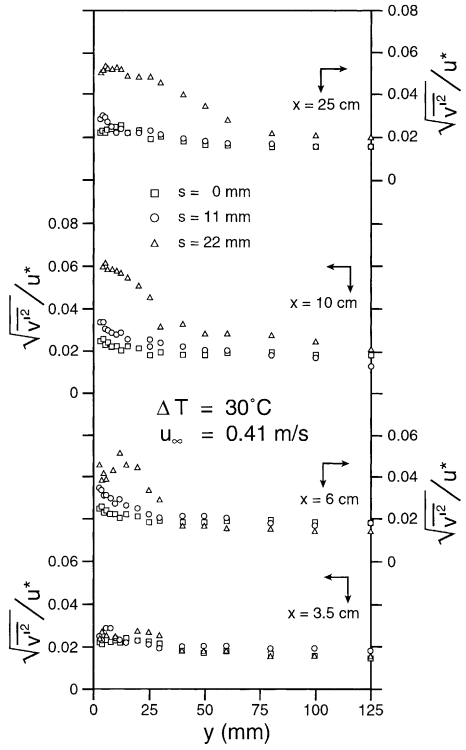

Fig. 9. Distributions of dimensionless transverse velocity fluctuation downstream of the step.

The dimensionless turbulent intensities of streamwise and transverse velocity and temperature fluctuations downstream from the step are presented in Figs. 8–10, respectively. As can be seen from these figures the values of the streamwise and transverse velocity and temperature fluctuations increase to a maximum as the distance from the heated wall increases, start to decrease as the distance from the heated wall continues to increase, and then reach a minimum value at the edge of the boundary-layer. For the flat plate case ($s = 0$ mm), Abu-Mulaweh et al. (2000) and Hattori et al. (2001) reported that introduction of small free stream velocity on turbulent natural convection flow suppresses turbulence and causes the flow to relaminarized. These figures, however, show that introduction of the step height enhances the turbulence intensity, which causes the flow to become turbulent downstream of the step. The existence of a backward-facing step triggers transition from the relaminarized flow upstream of the step to turbulent flow behind the step. The magnitudes of the intensities of both velocity and temperature fluctuations increase as the step height increases. This is caused by the larger impact angle of the upstream flow toward the heated plate downstream of the step as a result of the larger step height. The uncertainty in $\sqrt{\overline{u'^2}}/u^*$ and $\sqrt{\overline{v'^2}}/u^*$ is 6% and in $\sqrt{\overline{t'^2}}/\Delta T$ is 5%.

The nondimensional streamwise and transverse turbulent heat fluxes are presented in Figs. 11 and 12. It can be seen from the results that the general behavior of

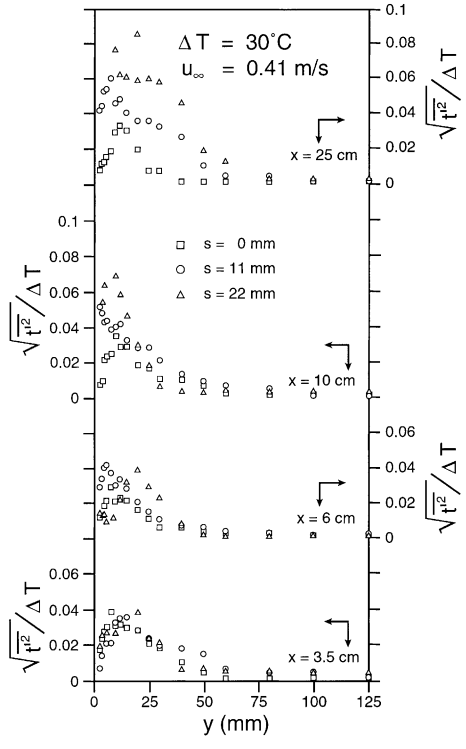

Fig. 10. Distributions of dimensionless temperature fluctuation downstream of the step.

both the streamwise and the transverse turbulent heat fluxes are the same with the streamwise magnitude being

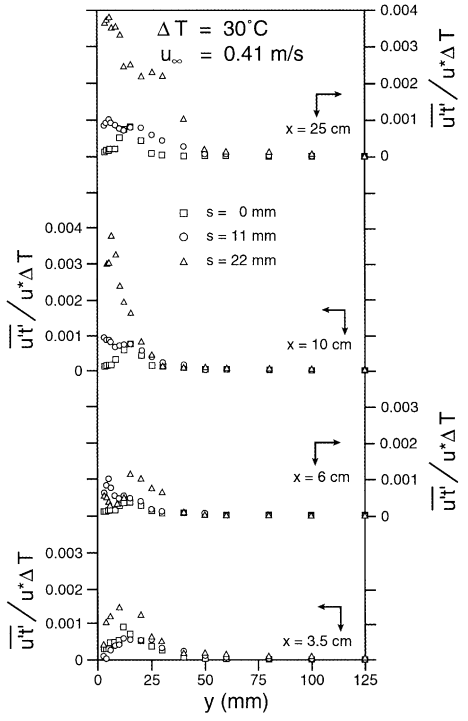

Fig. 11. Dimensionless streamwise turbulent heat flux distributions.

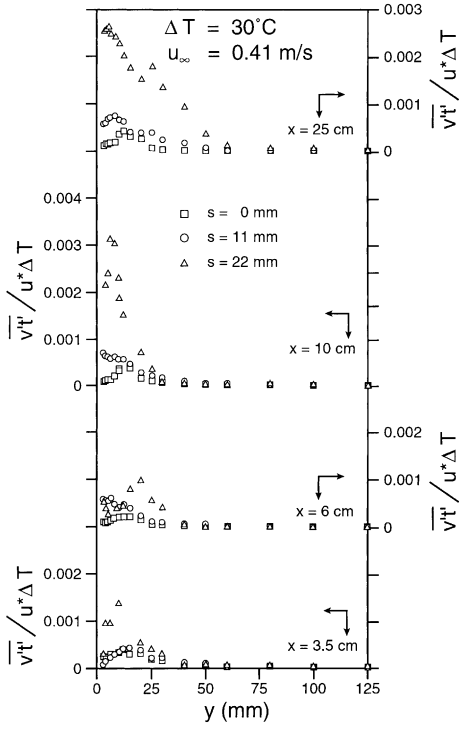

Fig. 12. Dimensionless transverse turbulent heat flux distributions.

larger. The magnitude increases rapidly to a maximum value near the wall and then decreases gradually as the free stream is approached. As can be seen from the figure, the values of turbulent heat fluxes increase with increasing step height. The uncertainty in $\overline{u't'}/u^*\Delta T$ and $\overline{v't'}/u^*\Delta T$ is 6%.

The convective heat transfer coefficients for the heated downstream wall were determined from the measured temperature distributions (temperature gradients) in the laminar sublayer near the heated wall. The air temperature was measured at four different locations within 0.5 mm from the heated wall in order to establish the temperature gradient at the heated wall. The temperature distributions in the laminar sublayer near the heated wall were linear and the temperature fluctuations in that region were very small (near zero). This technique for determining the surface temperature gradient and the convective heat transfer coefficient in turbulent flow was utilized and validated by Tsuji and Nagano (1988), Qiu et al. (1995), and Abu-Mulaweh et al. (1999, 2000). The effect of the step height on the local Nusselt number is illustrated in Fig. 13. As can be seen from the figure, the measured local Nusselt number downstream of the step (i.e., heat transfer rate from the heated downstream wall) increases with increasing step height. This is because the existence of a backward-facing step triggers transition from the relaminarized flow upstream of the step to turbulent flow downstream of the step. Increasing the step height enhances the turbulence intensity (as shown in Figs. 8–10) and results in an increase in the heat transfer rate. The location of the maximum heat transfer rate (i.e., the local Nusselt number) moves away from the step as the step height increases. This is because the maximum heat transfer rate occurs in the vicinity of the reattachment region where the velocity and temperature fluctuations are maximum and a larger step is associated with a larger reattachment length. It should be noted that for the case of flat plate ($s = 0$), the measured Nusselt number agrees well with the results reported by Hattori et al. (2001).

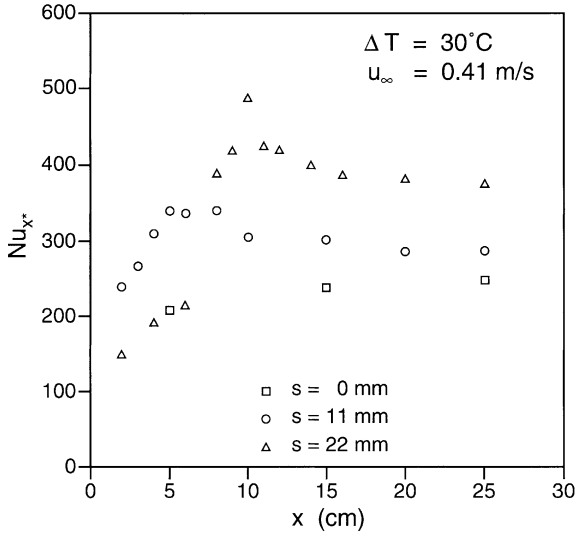

Fig. 13. Local Nusselt number variation downstream of the step.

The uncertainty in x is ± 1 mm and in the measured Nusselt number is $\pm 6\%$.

4. Conclusion

Detailed measurements of the flow and thermal fields in turbulent natural and mixed convection flows adjacent to a vertical, two-dimensional backward-facing step are reported. The present results reveal that increasing the step height enhances the turbulence intensity, which causes the flow to become turbulent downstream of the step. This is because the existence of a backward-facing step triggers transition from the relaminarized flow upstream of the step to turbulent flow downstream of the step. The turbulence intensity of both streamwise and transverse velocity fluctuations, the intensity of temperature fluctuations, and heat transfer rate downstream of the step are found to increase as the step height increases. Also, it was found that the reattachment length increases with increasing step height. As a result of the increase in the reattachment length, the location of the maximum heat transfer rate moves away from the step as the step height increases.

Acknowledgements

The present study was supported in part by grants from the National Science Foundation (NSF CTS-9304485) and Indiana Purdue University Fort Wayne (IPFW).

References

Abe, K., Kondoh, T., Nagano, Y., 1994. A new turbulence model for predicting fluid flow and heat transfer in separating and reattaching flows—I. Flow field calculations. International Journal of Heat and Mass Transfer 37 (1), 139–151.

Abe, K., Kondoh, T., Nagano, Y., 1995. A new turbulence model for predicting fluid flow and heat transfer in separating and reattaching flows—II. Thermal field calculations. International Journal of Heat and Mass Transfer 38 (8), 1467–1481.

Abu-Mulaweh, H.I., Armaly, B.F., Chen, T.S., 1995. Laminar natural convection flow over a vertical backward-facing step. Journal of Heat Transfer 117 (4), 895–901.

Abu-Mulaweh, H.I., Chen, T.S., Armaly, B.F., 1999. Turbulent natural convection flow over a backward-facing step. Experimental Heat Transfer 12 (4), 295–308.

Abu-Mulaweh, H.I., Chen, T.S., Armaly, B.F., 2000. Effects of free stream velocity on turbulent natural convection flow along a vertical plate. Experimental Heat Transfer 13 (3), 183–195.

Abu-Mulaweh, H.I., Armaly, B.F., Chen, T.S., 2001. Turbulent mixed convection flow over a backward-facing step. International Journal of Heat and Mass Transfer 44 (14), 2661–2669.

Hattori, Y., Tsuji, T., Nagano, Y., Tanaka, N., 2001. Effects of freestream on turbulent combined convection boundary layer along a vertical heated plate. International Journal of Heat and Fluid Flow 22, 315–322.

Hong, B., Armaly, B.F., Chen, T.S., 1993. Laminar mixed convection in a duct with a backward-facing step—The effects of inclination angle and Prandtl number. International Journal of Heat and Mass Transfer 36 (12), 3059–3067.

Inagaki, T., 1994. Heat transfer and fluid flow of turbulent natural convection along a vertical flat plate with a backward-facing step. Experimental Heat Transfer 7, 285–301.

Lin, J.T., Armaly, B.F., Chen, T.S., 1990. Mixed convection in buoyancy-assisting vertical backward-facing step flows. International Journal of Heat and Mass Transfer 33 (10), 2121–2132.

Moffat, R.J., 1988. Describing the uncertainties in experimental results. Experimental Thermal and Fluids Sciences 1, 3–17.

Park, T.S., Sung, H.J., 1995. A nonlinear low-Reynolds-number k–ϵ model for turbulent separated and reattaching flows—I. Flow field calculations. International Journal of Heat and Mass Transfer 38 (14), 2657–2666.

Qiu, S., Simon, T.W., Volino, R.J., 1995. Evaluation of local wall temperature heat flux and convective heat transfer. Coefficient from the near-wall temperature profile. ASME HTD 318, 45–52.

Rhee, G.H., Suung, H.J., 1996. A nonlinear low-Reynolds-number k–ϵ model for turbulent separated and reattachingflows—II. Theremal field calculations. International Journal of Heat and Mass Transfer. 39 (16), 3465–3474.

Vogel, J.C., Eaton, J.K., 1985. Combined heat and fluid dynamics measurements downstream of a backward-facing step. Journal of Heat Transfer 107 (4), 922–929.

Tsuji, T., Nagano, Y., 1988. Characteristics of a turbulent natural convection boundary layer along a vertical flat plate. International Journal of Heat and Mass Transfer 31 (8), 1723–1734.